

Heavy quark potential at finite imaginary chemical potential

Junichi Takahashi*, Takahiro Sasaki, Masanobu Yahiro

Department of Physics, Graduate School of Sciences, Kyushu University, Fukuoka 812-8581, Japan

E-mail: takahashi@phys.kyushu-u.ac.jp

Keitaro Nagata

KEK Theory Center, High Energy Accelerator Research Organization (KEK), Tsukuba 305-0801, Japan

Takuya Saito

Integrated Information Center, Kochi University, Kochi 780-8520, Japan

Hiroaki Kouno

Department of Physics, Saga University, Saga 840-8502, Japan

Atsushi Nakamura

Research Institute for Information Science and Education, Hiroshima University, Higashi-Hiroshima 739-8527, Japan

We investigate chemical-potential (μ) dependence of static-quark free energies in both the real and imaginary μ regions, using the clover-improved two-flavor Wilson fermion action and the renormalization-group improved Iwasaki gauge action. Static-quark potentials are evaluated from the Polyakov-loop correlator in the deconfinement phase and the imaginary $\mu = i\mu_I$ region and extrapolated to the real μ region with analytic continuation. As the analytic continuation, the potential calculated at imaginary $\mu = i\mu_I$ is expanded into a Taylor-expansion series of $i\mu_I/T$ up to 4th order and the pure imaginary variable $i\mu_I/T$ is replaced by the real one μ_R/T . At real μ , the 4th-order term weakens μ dependence of the potential sizably. Also, the color-Debye screening mass is extracted from the color-singlet potential at imaginary μ , and the mass is extrapolated to real μ by analytic continuation. The screening mass thus obtained has stronger μ dependence than the prediction of the leading-order thermal perturbation theory at both real and imaginary μ . This talk is based on [1].

31st International Symposium on Lattice Field Theory - LATTICE 2013

July 29 - August 3, 2013

Mainz, Germany

*Speaker.

1. Introduction

The free energies between two static quarks are fundamental quantities to understand inter-quark interactions. Particularly above T_{pc} , the static-quark potentials determined from the free energies characterize quark-gluon dynamics in QGP; for example, the inverse of the range of the color-singlet potential is the color-Debye screening mass. The potential largely affects the behavior of heavy-quark bound states such as J/Ψ and Υ in QGP created at the center of heavy-ion collisions [2]. In lattice QCD(LQCD) simulations, the static-quark potential is determined from the Polyakov-loop correlation function. For zero chemical potential, T dependence of the static-quark potential was investigated by quenched QCD [3, 4, 5] and full QCD with staggered-type [6] and Wilson-type quark actions [7, 8, 9]. For small μ/T , it was analyzed by the Taylor-expansion method with staggered-type [10] and Wilson-type quark actions [11]. In the analysis [11], the expansion coefficients are taken up to 2nd order of μ/T .

In this report, we present μ dependence of the static-quark free energies and the color-Debye screening mass in both the imaginary and real μ regions, performing LQCD simulations at imaginary μ and extrapolating the result to the real $\mu = \mu_{\text{R}}$ region with analytic continuation. We consider two temperatures above T_{pc} , i.e., $T/T_{\text{pc}} = 1.20$ and 1.35 . Following the previous LQCD simulation [11] at small μ/T , we compute static-quark free energies along the line of constant physics at $m_{\text{PS}}/m_{\text{V}} = 0.80$. As the analytic continuation, the static-quark potential at imaginary $\mu = i\mu_{\text{I}}$ is expanded into a Taylor-expansion series of $i\mu_{\text{I}}/T$ and pure imaginary variable $i\mu_{\text{I}}/T$ is replaced by real one μ_{R}/T . In the present work the Taylor-expansion coefficients of the static-quark potential are evaluated up to 4th order, whereas the coefficients were computed up to 2nd order in Ref. [11]. It is found that the 4th-order term yields non-negligible contributions to μ dependence of the static-quark potentials at real μ . At long distance, all of the color singlet and non-singlet potentials tend to twice the single-quark free energy, indicating that the interactions between heavy quarks are fully color-screened. Although this property is known for finite T and zero μ [8], the present work shows that the property persists also for imaginary μ . For imaginary μ , the color-singlet $q\bar{q}$ and the color-antitriplet qq interaction are attractive, whereas the color-octet $q\bar{q}$ and the color-sextet qq interaction are repulsive. The color-Debye screening mass at imaginary μ is extracted from the color-singlet potential there. The mass at real μ is extrapolated from the mass at imaginary μ by analytic continuation, i.e., by expanding the mass at imaginary μ into a power series of $i\mu_{\text{I}}/T$ up to 2nd order and replacing $i\mu_{\text{I}}$ by μ_{R} . The (μ/T) dependence of the screening mass is found to be stronger than the prediction of the leading-order thermal perturbation theory.

2. Static-quark free energies

The Polyakov loop is defined as

$$L(\mathbf{x}) = \prod_{t=1}^{N_t} U_4(\mathbf{x}, t) \quad (2.1)$$

with link variables $U_\mu \in \text{SU}(3)$. At imaginary μ , the ensemble average of the Polyakov loop becomes a complex number, $\langle \text{Tr}L(0) \rangle \equiv \Phi e^{i\theta}$. The modulus is related to the single-quark free

energy F_q as $\Phi = \exp[-F_q/T]$. After an appropriate gauge fixing, one can derive the static-quark free energies (potentials) V_M of color channel M from the Polyakov-loop correlator [12, 13]:

$$e^{-V_1(r,T,\mu)/T} = \frac{1}{3} \langle \text{Tr} L^\dagger(\mathbf{x}) L(\mathbf{y}) \rangle, \quad (2.2)$$

$$e^{-V_8(r,T,\mu)/T} = \frac{1}{8} \langle \text{Tr} L^\dagger(\mathbf{x}) \text{Tr} L(\mathbf{y}) \rangle - \frac{1}{24} \langle \text{Tr} L^\dagger(\mathbf{x}) L(\mathbf{y}) \rangle, \quad (2.3)$$

$$e^{-V_{3^*}(r,T,\mu)/T} = \frac{1}{6} \langle \text{Tr} L(\mathbf{x}) \text{Tr} L(\mathbf{y}) \rangle - \frac{1}{6} \langle \text{Tr} L(\mathbf{x}) L(\mathbf{y}) \rangle, \quad (2.4)$$

$$e^{-V_6(r,T,\mu)/T} = \frac{1}{12} \langle \text{Tr} L(\mathbf{x}) \text{Tr} L(\mathbf{y}) \rangle + \frac{1}{12} \langle \text{Tr} L(\mathbf{x}) L(\mathbf{y}) \rangle, \quad (2.5)$$

where $r = |\mathbf{x} - \mathbf{y}|$ and the subscripts $M = (1, 8, 3^*, 6)$ mean the color-singlet, -octet, -antitriplet and -sextet channels, respectively. We adopt the Coulomb gauge fixing.

In general, the V_M ($M = 1, 8, 3^*, 6$) are complex at finite imaginary μ . The real part of V_M is \mathcal{C} -even and the imaginary part is \mathcal{C} -odd. This can be easily understood by expanding V_M into a power series of $i\mu_I/T$:

$$\frac{V_M(r, T, \mu_I)}{T} = v_0(r) + iv_1(r) \left(\frac{\mu_I}{T} \right) + v_2(r) \left(\frac{\mu_I}{T} \right)^2 + iv_3(r) \left(\frac{\mu_I}{T} \right)^3 + v_4(r) \left(\frac{\mu_I}{T} \right)^4, \quad (2.6)$$

where we consider terms up to 4th order. The potential V_M at real μ is obtained from that at imaginary μ by analytic continuation, i.e., by replacing $i\mu_I/T$ by μ_R/T :

$$\frac{V_M(r, T, \mu_R)}{T} = v_0(r) + v_1(r) \left(\frac{\mu_R}{T} \right) - v_2(r) \left(\frac{\mu_R}{T} \right)^2 - v_3(r) \left(\frac{\mu_R}{T} \right)^3 + v_4(r) \left(\frac{\mu_R}{T} \right)^4. \quad (2.7)$$

The WHOT-QCD Collaboration calculated the Taylor-expansion coefficients of V_M up to 2nd order by using the Taylor-expansion method and the reweighting technique with the Gaussian approximation for the distribution of the complex phase of the quark determinant [11]. In this work, meanwhile, we obtain the coefficients up to 4th order from V_M at imaginary μ by expanding it as in (2.6).

3. Results of the lattice simulations and the analytic continuation

We employ the clover-improved two-flavor Wilson fermion action and the renormalization-group improved Iwasaki gauge action. Finite temperature simulations are performed on $16^3 \times 4$ lattices along the line of constant physics with $m_{\text{PS}}/m_V = 0.80$. We consider two temperatures $T/T_{\text{pc}} = 1.20$ and 1.35 . We generated 16,000 trajectories and removed the first 1,000 trajectories as thermalization for all the parameter set. We measured the static-quark potential at every 100 trajectories.

The coefficients $v_2(r)$ and $v_4(r)$ of $V_1(r)$ are shown in Fig. 1. The ratio $v_4(r)/v_2(r)$ is about $3/4$ for $T/T_{\text{pc}} = 1.20$ and about $1/4$ for $T/T_{\text{pc}} = 1.35$. Thus the contribution of $v_4(r)$ to $V_1(r)$ is significant near T_{pc} such as $T/T_{\text{pc}} = 1.20$. Even at higher T such as $T/T_{\text{pc}} = 1.35$, the contribution is not negligible.

Figure 2 shows the color-singlet potential at imaginary and real μ for (a) $T/T_{\text{pc}} = 1.20$ and (b) $T/T_{\text{pc}} = 1.35$. The chemical potential is varied from $(\mu/T)^2 = -1.0$ to 1.0 . The potential V_1 is \mathcal{C} -even, so that $v_1(r) = v_3(r) = 0$. Furthermore, if $v_4(r) = 0$, the potential V_1/T will linearly

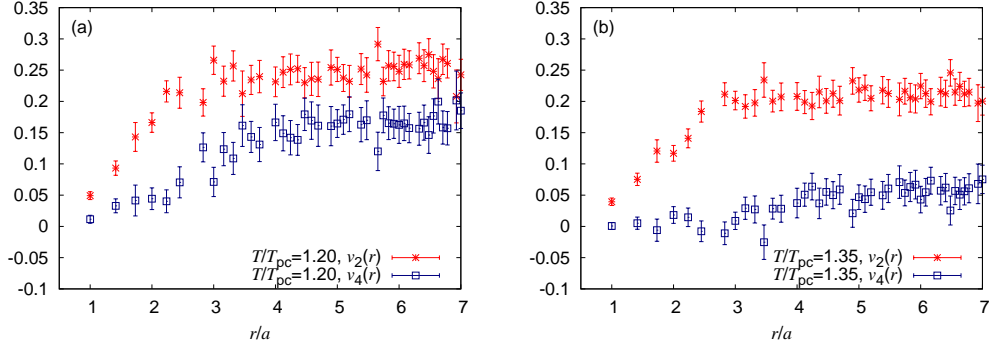


Figure 1: Taylor-expansion coefficients, $v_2(r)$ and $v_4(r)$, of $V_1(r)$ at (a) $T/T_{pc} = 1.20$ and (b) $T/T_{pc} = 1.35$.

depend on $(\mu/T)^2$. For $T/T_{pc} = 1.20$, $v_4(r)$ is comparable to $v_2(r)$. For this property, in panel (a) of Fig. 2, μ/T dependence of V_1/T is much weaker at real μ than at imaginary μ . In panel (b) of $T/T_{pc} = 1.35$, $v_4(r)$ is still non-negligible compared with $v_2(r)$, so that V_1/T has still weaker μ/T dependence at real μ than at imaginary μ .

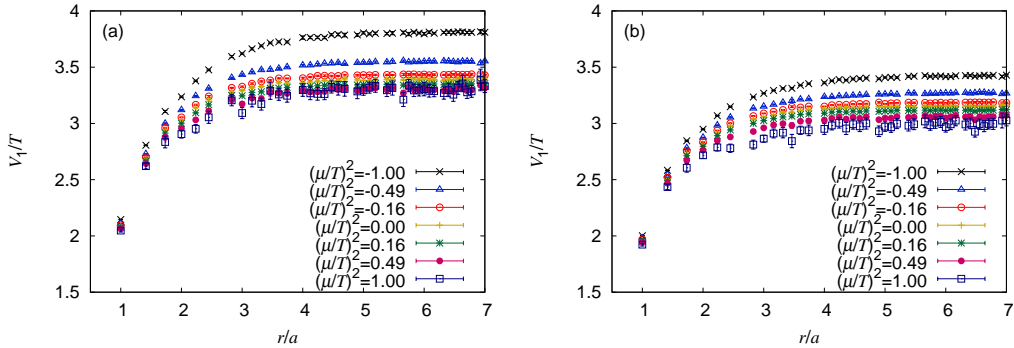


Figure 2: μ/T dependence of the color-singlet $q\bar{q}$ potential for (a) $T/T_{pc} = 1.20$ and (b) $T/T_{pc} = 1.35$.

For the case of $T > T_{pc}$ and $\mu = 0$, the potentials $V_M(r)$ are known to tend to twice the single-quark free energy $2F_q$ in the limit of large r [8]. This behavior persists also for imaginary μ . The interactions between heavy quarks are thus color screened also for imaginary μ . Following the previous works [8, 4, 5, 9, 11], we then subtract $2F_q$ from $V_M(r)$. The subtracted static-quark potentials are shown in Fig. 3(a) for the color-singlet and -octet channels and in Fig. 3(b) for the color-antitriplet and -sextet channels. Needless to say, the physical interpretation of gauge dependent quantities is not straightforward; this is the case also for the potentials. See ref. [14]. Our results show distinctively different behaviors for the singlet/antitriplet channel and the octet/sextet channel; the former is "attractive" and the latter is "repulsive". The attractive interactions have strong μ_I/T dependence, but the repulsive interactions have weak μ_I/T dependence.

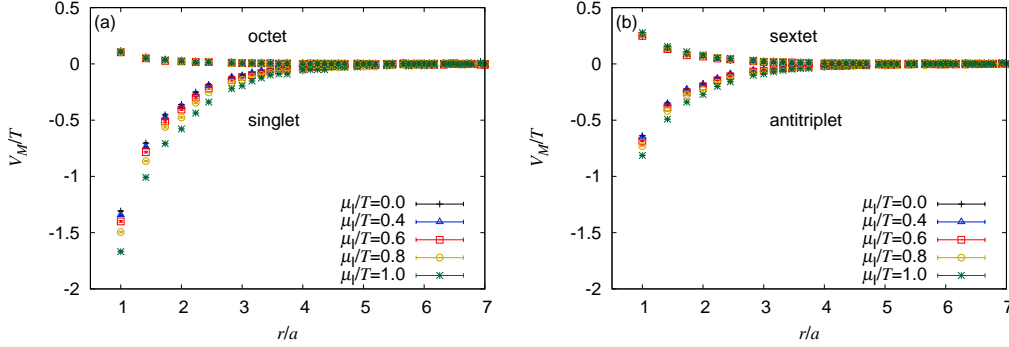


Figure 3: μ_i/T dependence of the subtracted $q\bar{q}$ in (a) the color-singlet and -octet channels and qq potentials in (b) the color-antitriplet and -sextet channels at $T/T_{pc} = 1.20$.

4. Color-Debye screening mass

In order to analyze the color screening effect, we fit the static-quark potential to the screened Coulomb form

$$V_M(r, T, \mu) = C_M \frac{\alpha_{\text{eff}}(T, \mu)}{r} e^{-m_D(T, \mu)r}, \quad (4.1)$$

where $C_M \equiv \langle \sum_{a=1}^8 t_1^a \cdot t_2^a \rangle_M$, α_{eff} and $m_D(T, \mu)$ are the Casimir factor, the effective running coupling and the color-Debye screening mass, respectively. Here, we focus our discussion on the color-singlet channel that is most important in the real world, and the Casimir factor in the singlet channel is $C_1 = -4/3$. Since $V_1 = 0$ in the limit of large r in (4.1), we extract the screening mass from the subtracted static-quark potential. Following the previous work [9], we choose a fit range of $\sqrt{11} \leq r/a \leq 6.0$.

In the leading-order (LO) hard thermal loop (HTL) perturbation theory, the color-Debye screening mass is obtained [15] by

$$\frac{m_D(T, \mu)}{T} = g_{2l}(v) \sqrt{\left(1 + \frac{N_f}{6}\right) + \frac{N_f}{2\pi^2} \left(\frac{\mu}{T}\right)^2} \quad (4.2)$$

with the 2-loop running coupling g_{2l} given by

$$g_{2l}^{-2}(v) = \beta_0 \ln\left(\frac{v}{\Lambda}\right)^2 + \frac{\beta_1}{\beta_0} \ln \ln\left(\frac{v}{\Lambda}\right)^2, \quad (4.3)$$

where the argument in the logarithms is rewritten into $v/\Lambda = (v/T)(T/T_{pc})(T_{pc}/\Lambda)$ with $\Lambda = \Lambda_{\overline{\text{MS}}}^{N_f=2} \simeq 261$ MeV [16] and $T_{pc} \simeq 171$ MeV [17], and the renormalization point v is assumed to be $v = \sqrt{(\pi T)^2 + \mu^2}$ [18].

Figure 4 shows the $(\mu/T)^2$ dependence of the color-Debye screening mass for (a) $T/T_{pc} = 1.20$ and (b) $T/T_{pc} = 1.35$. The lattice-simulation results are plotted by the cross symbols. The screening mass is then expanded up to 2nd order of μ/T :

$$\frac{m_D}{T} = a_0(T) + a_2(T) \left(\frac{\mu}{T}\right)^2, \quad (4.4)$$

where note that m_D is \mathcal{C} -even and hence it has no linear term of μ/T . The screening mass at real μ is extrapolated from that at imaginary μ by using (4.4).

The results of the extrapolation, represented by the hatching area, are consistent with the previous LQCD result, denoted by a circle symbol, at $\mu = 0$ [9] for both cases of $T/T_{pc} = 1.20$ and 1.35. Comparing the hatching area (the result of the extrapolation) with the solid line (the prediction of the leading-order thermal perturbation theory), one can see that the present LQCD results show stronger μ/T dependence than the prediction of the perturbation theory.

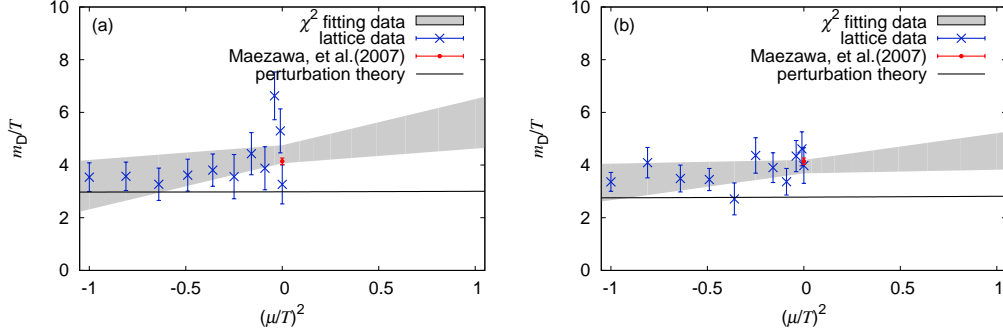


Figure 4: $(\mu/T)^2$ dependence of the color-Debye screening mass for (a) $T/T_{pc} = 1.20$ and (b) 1.35. The screening mass is determined from the singlet potential. Crosses with error bars denote results of the present lattice simulations at imaginary μ , while a circle with an error bar is a result of the previous lattice simulations at $\mu = 0$ [9].

5. Summary

We have investigated μ dependence of the static-quark potential and the color-Debye screening mass in both the imaginary and real μ regions, performing LQCD simulations at imaginary μ and extrapolating the result to the real μ region with analytic continuation. LQCD calculations are done on a $16^3 \times 4$ lattice with the clover-improved two-flavor Wilson fermion action and the renormalization-group improved Iwasaki gauge action. We took an intermediate quark mass and considered two cases of $T/T_{pc} = 1.20$ and 1.35.

The static-quark potential at real μ was obtained by expanding the potential at imaginary μ into a Taylor-expansion series of $i\mu_I/T$ up to 4th order and replacing $i\mu_I$ to μ_R . Since the expansion series was taken only up to 2nd order in the previous analysis [11], this is the first analysis that investigates contributions of the 4th-order term to the potential. We found that at real μ the 4th-order term weakens μ dependence of the potential sizably. This effect becomes more significant as T decreases toward T_{pc} . We have also investigated color-channel dependence of the static-quark potentials. At large distance, all the potentials tend to twice the single-quark free energy, indicating that the interactions are fully color screened. Although this property is known for finite T and zero μ [8], the present analysis shows that the property persists also for imaginary μ . For imaginary μ , the color-singlet $q\bar{q}$ and the color-antitriplet qq interaction are attractive, whereas the color-octet $q\bar{q}$ and the color-sextet qq interaction are repulsive.

The color-Debye screening mass is evaluated from the color-singlet potential at imaginary μ . The screening mass thus obtained at imaginary μ is extrapolated to real μ by expanding the mass at imaginary μ into a power series of $i\mu_I/T$ up to 2nd order and replacing $i\mu_I/T$ by μ_R/T . The resulting mass has stronger μ dependence at both imaginary and real μ than the prediction of the leading-order thermal perturbation theory.

Acknowledgments

Junichi Takahashi is supported by JSPS KAKENHI (No. 25-3944), Takahiro Sasaki by JSPS KAKENHI (No. 23-2790), Atsushi Nakamura by JSPS KAKENHI (Nos. 23654092, 24340054) and Takuya Saito by JSPS KAKENHI (No. 23740194). Keitaro Nagata is supported in part by Strategic Programs for Innovative Research (SPIRE) Field 5. The numerical calculations were performed on NEC SX-9 and SX-8R at CMC, Osaka University.

References

- [1] J. Takahashi et al., arXiv:1308.2489 [hep-lat], (2013).
- [2] T. Matsui and H. Satz, Phys. Lett. B **178**, 416 (1986).
- [3] O. Kaczmarek, F. Karsch, E. Laermann, and M. Lutgemeier, Phys. Rev. D **62**, 034021 (2000).
- [4] A. Nakamura, and T. Saito, Prog. Theor. Phys. **111**, 733 (2004).
- [5] A. Nakamura, and T. Saito, Phys. Lett. B **621** 171 (2005).
- [6] O. Kaczmarek, and F. Zantow, Phys. Rev. D **71**, 114510 (2005).
- [7] V. G. Bornyakov et al. (DIK Collaboration), Phys. Rev. D **71**, 114504 (2005).
- [8] Y. Maezawa et al. (WHOT-QCD Collaboration), arXiv:1112.2756 [hep-lat], (2012).
- [9] Y. Maezawa et al. (WHOT-QCD Collaboration), Phys. Rev. D **75**, 074501 (2007).
- [10] M. Döring, S. Ejiri, O. Kaczmarek, F. Karsch, and E. Laermann, Eur. Phys. J. C **46**, 179 (2006).
- [11] S. Ejiri et al. (WHOT-QCD Collaboration), Phys. Rev. D **82**, 014508 (2010).
- [12] S. Nadkarni, Phys. Rev. D **33**, 3738 (1986).
- [13] S. Nadkarni, Phys. Rev. D **34**, 3904 (1986).
- [14] O. Jahn, and O. Philipsen, Phys. Rev. D **70**, 074504 (2004).
- [15] Michel Le Bellac, *Thermal Field Theory*, Cambridge University Press, Cambridge (1996).
- [16] M. Göckeler et al., Phys. Rev. D **73**, 014513 (2006).
- [17] A. Ali Khan et al. (CP-PACS Collaboration), Phys. Rev. D **63**, 034502 (2000).
- [18] A. Ipp, and A. Rebhan, J. High Energy Phys. **06** 032 (2003).